International Journal of Pharmaceutics, 16 (1983) 295–304
Elsevier

Dissolution at porous interfaces V. Pore effects in a parallel-plate dissolution cell

H. Grijseels * and C.J. de Blaey **

Department of Pharmaceutics, Subfaculty of Pharmacy, University of Utrecht, Catharijnesingel 60, 3511 GH Utrecht (The Netherlands)

(Received February 14th, 1983)
(Accepted March 23rd, 1983)

Summary

A parallel-plate dissolution cell is introduced as a method to study the effect of pores on the dissolution rate of a tablet surface.

By measuring the dissolution rate of a smooth surface under various flow conditions it is confirmed that the experimental behaviour of the cell complies with hydrodynamic theory. The value of the diffusion coefficient calculated from these results is equal to the one found in a previous rotating disk study.

The critical pore diameter that is obtained from dissolution experiments with porous surfaces in the cell is in full agreement with the value predicted on basis of the results with the rotating disk technique and the theoretically calculated friction velocity at the surfaces of the parallel-plate dissolution cell.

Introduction

Recently we reported on the use of a centrifugal stirrer apparatus (Grijseels and de Blaey, 1981), a rotating disk technique (Grijseels et al., 1983a and b) and a natural convection dissolution cell (Grijseels et al., 1983c) to investigate the effect of pores on the dissolution rate of a surface. In the present paper we describe a thin-layer flow cell to study the behaviour of pores in a parallel-plate poiseuille flow.

* Present address: Cedona Pharmaceuticals B.V., P.O. Box 850, 2003 RW Haarlem, The Netherlands.
** To whom correspondence should be addressed.

Theoretical background

For a surface with length, ℓ, and width, b, dissolving in a poiseuille flow between two parallel plates the convective diffusion theory of Levich (1962) provides the possibility to predict the theoretical dissolution rate. Under sink conditions the following equation is valid (Grijseels et al., 1981):

$$R = 1.47\, C_s \cdot D^{2/3} \left(\frac{\bar{u}}{d} \right)^{1/3} b \cdot \ell^{2/3} \qquad (1)$$

For convenience all symbols are listed in Table 1. Shah and Nelson (1975) found a quite satisfactory agreement between this theoretical equation and experiments performed in a parallel-plate cell, when they varied solubility, diffusion coefficient, flow rate and surface dimensions.

A variety of cells based on the same hydrodynamic principles were developed in

TABLE I

LIST OF SYMBOLS

Symbol	Explanation	Units
b	width of dissolving surface	(m)
c	distance from leading edge of surface in direction of flow	(m)
C_s	solubility	$(kg \cdot m^{-3})$
d	distance between parallel plates	(m)
d_{crit}	critical pore diameter	(m)
D	diffusion coefficient	$(m^2 \cdot s^{-1})$
H	length of inlet section	(m)
k_1	constant	
ℓ	length of dissolving surface	(m)
L	length of conduit	(m)
P	pressure	$(N \cdot m^{-2})$
P	probability	
Q	flow	$(m^3 \cdot s^{-1})$
R	dissolution rate	$(kg \cdot s^{-1})$
Re	Reynolds number	
S.D.	standard deviation	
u	velocity	$(m \cdot s^{-1})$
$\bar{u}$	mean velocity in flow direction	$(m \cdot s^{-1})$
u_{max}	maximum velocity in flow direction	$(m \cdot s^{-1})$
v_f	friction velocity	$(m \cdot s^{-1})$
w	width of flow channel	(m)
x	distance in flow direction	(m)
y	distance normal to parallel plates	(m)
ΔP	driving pressure	$(N \cdot m^{-2})$
ΔR	increase of the dissolution rate per pore	$(kg \cdot s^{-1})$
η	dynamic viscosity	$(kg \cdot m^{-1} \cdot s^{-1})$
ν	kinematic viscosity	$(m^2 \cdot s^{-1})$
ρ	fluid density	$(kg \cdot m^{-3})$
τ_0	shear stress	$(N \cdot m^{-2})$

electrochemical studies. Swartzfager (1976) and Ikenoya et al. (1978) found values of 0.33 and 0.3, respectively, for the exponent in the relationship between mass transfer and flow rate. Brunt and Bruins (1979) erroneously applied the Levich equation for convective diffusion at a semi-infinite plate to their thin-layer cell and therefore expected a square- instead of a cube-root relationship between mass flux and flow rate. However, their data also are fitted better by a value of about 0.3 for the exponent of $\bar{u}$.

Hydrodynamics in the dissolution cell (Fig. 1)

The laminar fluid flow between two parallel plates separated by a distance, d, is characterized by a parabolic velocity profile of the form (Beek and Muttzall, 1975):

$$u = u_{max}\left(1 - \left(\frac{2y - d}{d}\right)^2\right) \tag{2}$$

In such a poiseuille flow u_{max} is defined as:

$$u_{max} = \frac{\Delta P \cdot d^2}{8 \cdot \eta \cdot L} \tag{3}$$

where ΔP is the driving pressure across the conduit of length L. The laminar flow regimen between two plates can be divided in two regions. Next to the fully established poiseuille flow described by Eqn. 2, a so-called inlet-section H exists, where the hydrodynamic boundary layers are still growing before the equilibrium poiseuille state is reached (Grijseels et al., 1981). Van Wagenen and Andrade (1980) emphasize the importance of taking the length of the inlet-section into account during the design of a parallel-plate system. This length H can be computed from

$$H = k_1 \cdot d \cdot Re \tag{4}$$

Values of k_1 ranging from 0.013 to 0.05 are given by different authors (Bird et al., 1960; Levich, 1962; van Wagenen and Andrade, 1980). The length of H, calculated under the most extreme conditions during our experiments ($Q = 1.00$ ml $\cdot s^{-1}$, $d = 5.0$ mm, $k_1 = 0.05$), amounts to 9 mm, whereas the distance from the inlet port to the leading edge of the dissolving surface is over 150 mm. This ensures that the tablet surface is always exposed to a completely established poiseuille flow.

In a previous paper (Grijseels et al., 1983b) we reported on the influence of pores drilled into the surface of a rotating disk with respect to the hydrodynamics. It was established that the critical pore diameter, which is the diameter an individual pore must exceed to cause an increase of the dissolution rate, is inversely proportional to the friction velocity at the surface of the rotating disk:

$$d_{crit} = \frac{2.70}{v_f} \tag{5}$$

An important objective of the present study is to investigate whether the pore

effects observed with the rotating disk technique are transferable to other hydrodynamic systems. For that purpose knowledge of the size of the friction velocity at the surfaces of the parallel-plate cell is necessary. According to Beek and Muttzall (1975) the shear stress on the wall (y = 0) is given by:

$$\tau_0 = \frac{d}{2} \cdot \frac{dP}{dx} \tag{6}$$

Replacing dP/dx by $\Delta P/L$ and combining Eqns. 3 and 6, we find

$$\tau_0 = \frac{4 \cdot \eta \cdot u_{max}}{d} \tag{7}$$

Since in a poiseuille flow between two plates $u_{max} = 1.5 \cdot \bar{u}$ and $\bar{u} = \frac{Q}{w \cdot d}$, Eqn. 7 can be simplified to

$$\tau_0 = \frac{6 \cdot \eta \cdot Q}{w \cdot d^2} \tag{8}$$

The friction velocity at the wall is defined as $v_f = (\frac{\tau_0}{\rho})^{1/2}$ (Levich, 1962), and therefore

$$v_f = \sqrt{\frac{6 \cdot \nu \cdot Q}{w \cdot d^2}} \tag{9}$$

This equation allows us to calculate the friction velocity at the dissolving surface as a function of flow Q, kinematic viscosity ν and the dimensions of the flow cross-section, d and w.

Experimental

The flow cell is a modification of the dissolution cell designed by Shah and Nelson (1975). As can be seen in Fig. 1 the rectangular cell consists of two plastic plates which are tightened together by bolts and nuts. In the lower surface of the top plate a rectangular, 50 mm wide flow-channel is cut out. On both ends the flow-channel narrows gradually towards the circular in- and outlet ports.

The standard height of the channel is 2.0 mm, but by means of appropriate spacers the effective distance between top and bottom plate can be varied up to 12.0 mm. The dissolving compound is compressed to a tablet in a metal die, which can be installed in the bottom plate of the dissolution cell. The dissolving, rectangular surface of the tablet (30.5 × 15.2 mm) is flush with the surfaces of the die and the bottom plate. The die can be positioned in the cell in two different orientations: with the long axis of the dissolving surface either parallel or perpendicular to the direction of the flow.

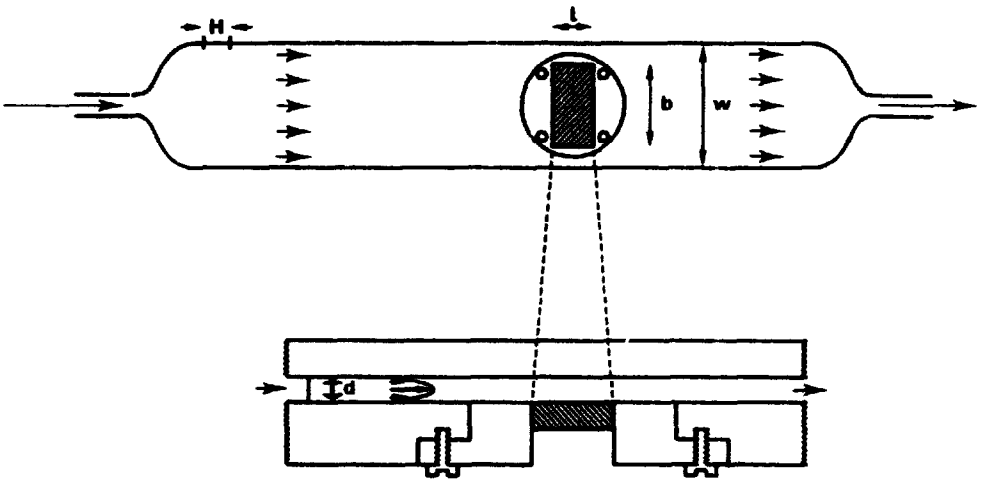

Fig. 1. Parallel-plate dissolution cell in top- and side-view. Symbols are explained in Table 1.

By means of a conventional flow system with a pump, constant head tanks and a flowmeter, demineralized water of $20.0 \pm 0.2°C$ was led through the dissolution cell at a constant flow rate. Freshly boiled water was used to avoid the occurrence of air bubbles in the flow system, that would disturb the poiseuille flow profile in the dissolution cell or affect the flow rate.

The cell was positioned to give a horizontal flow with the tablet surface dissolving in upward direction to minimize natural convection effects.

Nicotinic acid was chosen as test compound for the dissolution experiments. It was used as supplied and met the requirements of the European Pharmacopoeia (1975). The solubility of nicotinic acid in demineralized water was determined previously (Grijseels et al., 1983a) as 15.4 $kg \cdot m^{-3}$ (at 20.0°C). In the same study we measured a value of 0.72×10^{-9} $m^2 \cdot s^{-1}$ for its diffusion coefficient by means of the rotating disk technique.

Via a spectrophotometer, where the absorbance was measured at a wave length of 259 nm, the effluent was led to a sink. A microcomputer collected the output signal of the spectrophotometer 50 times every 10 s and computed and stored the mean value. After the surface was wetted, the dissolution process stabilized in 2–3 min. The mean dissolution rate was calculated from the combination of the flow rate and the concentration data collected between 5 and 15 min after the start of the experiment.

Calibration was achieved by running a standard solution through the spectrophotometer. All experiments were performed in triplicate to allow further statistical calculations.

Results and Discussion

Compliance with theory

To test whether our parallel-plate cell complied with theory, we measured the

dissolution rate of intact tablet surfaces as a function of the fluid flow (Q = 0.40, 0.56, 0.67 or 1.00 ml · s^{-1}), the orientation of the tablet (ℓ = 30.5 mm and b = 15.2 mm or vice versa) and the channel height (d = 2.0 or 5.0 mm). According to Eqn. 1, a plot of the dissolution rate versus $(\bar{u})^{1/3} \cdot d^{-1/3} \cdot b \cdot \ell^{2/3}$ should give a straight line with slope $1.47 \cdot C_s \cdot D^{2/3}$. Fig. 2 shows that a linear relationship indeed exists. Moreover, using the values of C_s and D determined previously in rotating disk studies, the theoretically predicted line was also drawn in Fig. 2. Clearly the compliance of the cell with the hydrodynamic theory is very good.

By means of linear regression, analysis of the experimental data a value of 0.71×10^{-9} $m^2 \cdot s^{-1}$ was computed for the diffusion coefficient, D. This value is in excellent agreement with the value of 0.72×10^{-9} $m^2 \cdot s^{-1}$ determined in the rotating disk apparatus.

Critical pore diameter

In previous rotating disk studies it was found that cylindrical pores in a surface can increase the dissolution rate of that surface, provided that the pore diameter exceeds a certain critical value. For relatively deep pores, with a depth : diameter ratio over 1.5, the increase of the dissolution rate due to one pore, ΔR, appeared to be directly proportional to the difference in actual and critical pore diameter. Fig. 3 shows the surface of a tablet with pores drilled side by side perpendicular to the flow direction. During the dissolution experiments troughs develop downstream of each pore due to enhanced erosion as a consequence of the provoked turbulence. The development of the trough is measured as an increased dissolution rate and Fig. 4 demonstrates that in the parallel-plate flow pores behave essentially the same as in a

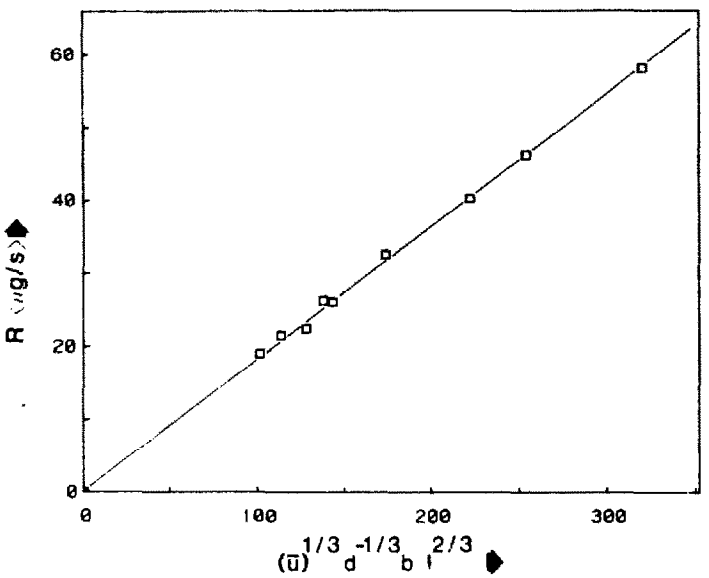

Fig. 2. Dissolution rate of a smooth nicotinic acid surface at different hydrodynamic conditions. The squares represent experimental data; all standard deviations fall within the drawn symbols. The drawn line is predicted theoretically.

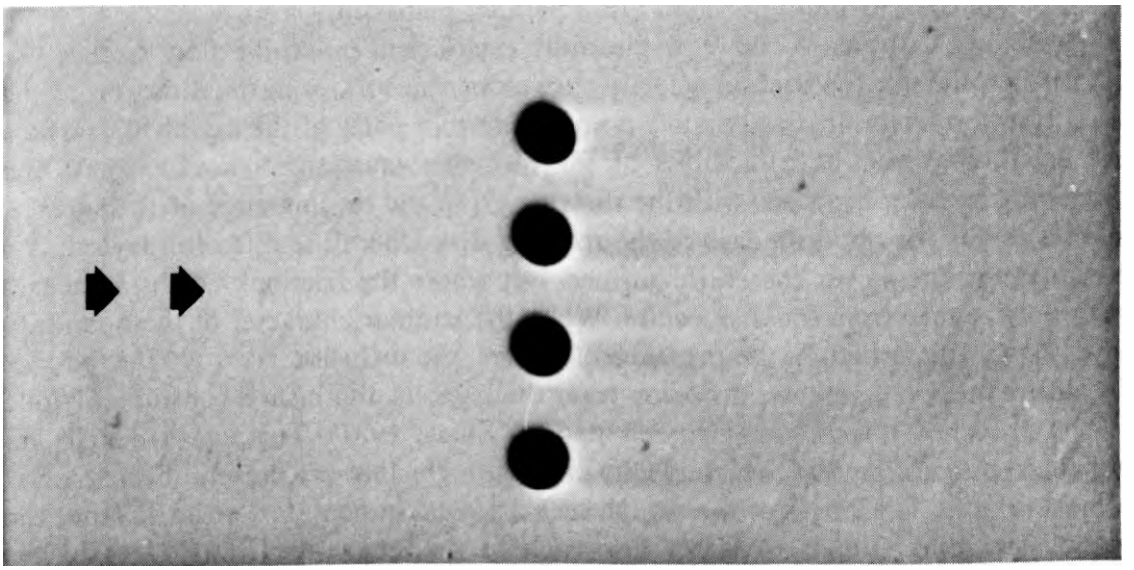

Fig. 3. Photograph of the surface of a nicotinic acid tablet after a dissolution experiment of about 30 min. Four pores with a diameter of 1.50 mm were drilled side by side in the tablet surface.

rotating disk surface. Least-squares regression analysis of the data in Fig. 4 gives a value for the critical pore diameter of 0.51 ± 0.05 mm.

By means of Eqn. 9 the friction velocity at the tablet surface was calculated: $v_f = 5.49$ mm · s^{-1} ($\nu = 1.004 \times 10^{-6}$ $m^2 \cdot s^{-1}$ at 20.0°C), and with the relationship in Eqn. 5 a value of 0.49 mm would have been predicted for d_{crit}. This remarkably good agreement leads to the conclusion that pores behave identically in the laminar

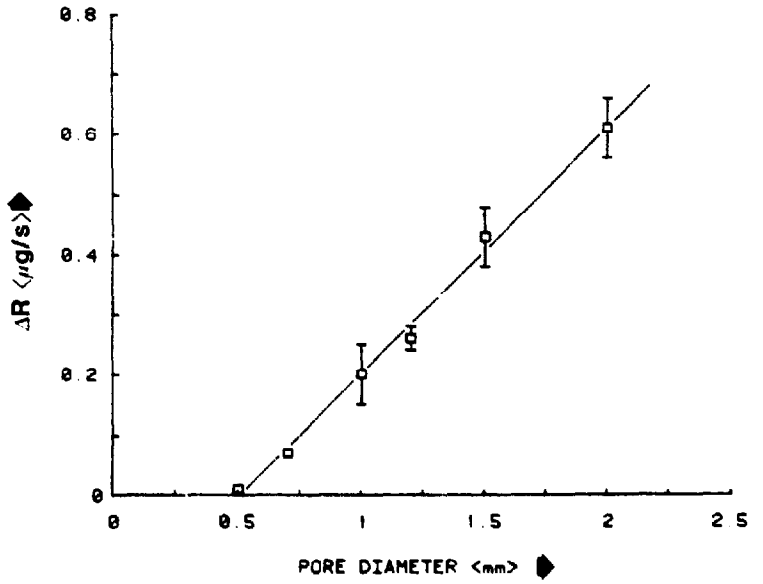

Fig. 4. Increase of the dissolution rate per pore (ΔR) as a function of the pore diameter. d = 2.0 mm; Q = 1.00 ml·s^{-1}; b = 15.2 mm; ℓ = 30.5 mm. The points are connected by the least-squares regression line. Vertical bars represent the standard deviation. If not shown they fall within the drawn symbol.

flow regimens at a rotating disk and in a parallel-plate cell.

According to Eqns. 2 and 9, in the fully established poiseuille flow neither the velocity profile nor the friction velocity vary along the surface in the direction of the fluid flow. So from a hydrodynamic point of view all parts of the dissolving surface are equal. However, the thickness of the diffusion layer, that develops past the dissolving surface, increases with the distance from the leading edge of the surface. In fact this is the opposite case of the rotating disk where the diffusion layer has a constant thickness over the entire surface, but where the friction velocity increases with the distance from the disk centre. When the laminar character of the boundary layer flow is disturbed by the presence of a pore, the diffusion layer is affected too. Downstream of the pore the diffusion layer thickness is diminished considerably due to the provoked turbulence (Grijseels and de Blaey, 1981). This causes locally an enhanced dissolution flux, which results in the troughs that are present in the eroded tablet surfaces. The length of the trough seems a good indication for the distance the turbulence zone extends. Another approach to determine the trough length was achieved by drilling pores at varying distances from the leading edge of the dissolving surface. In Fig. 5 the dissolution rate of a surface with pores is plotted versus the distance between the leading edge of the tablet surface and the pores which lie side by side downstream in the surface. The results demonstrate that irrespective of their position the pores give an increase of the dissolution rate with regard to a smooth surface (dashed line). The dissolution rate increase seems to be almost independent of the distance of the pores from the leading edge. Only in the case where the pores lie very close to the tailing edge of the surface (c = 29.5 mm) is the increase smaller, probably since the troughs end abruptly at the edge of the

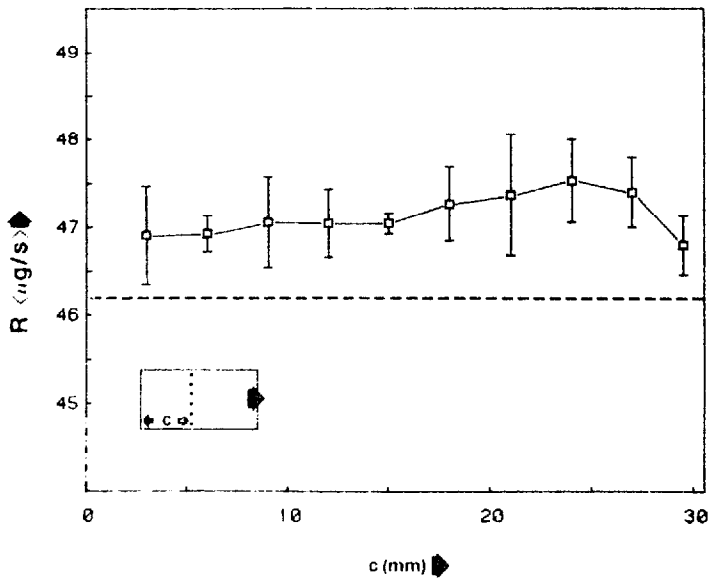

Fig. 5. Dissolution rate of a surface with pores versus the distance between the leading edge of the surface and the pores. d = 2.0 mm; Q = 1.00 ml·s^{-1}; b = 15.2 mm; ℓ = 30.5 mm; 6 pores (diameter 1.20 mm; depth 1.7 mm) situated side by side in the surface. Vertical bars represent the standard deviation.

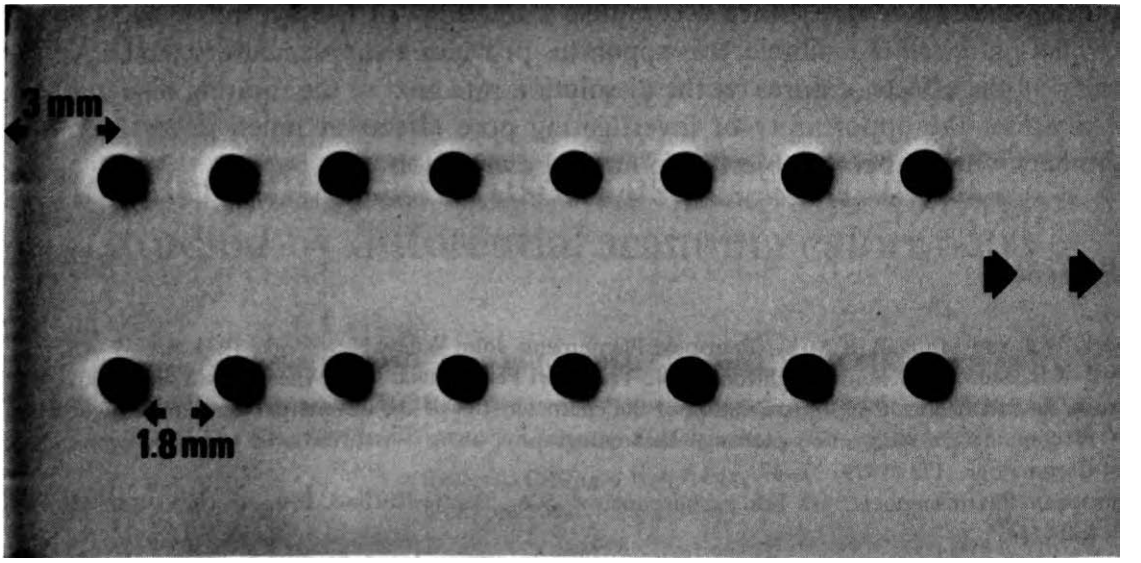

Fig. 6. Orientation of pores in experiments to determine the effective trough length; pore diameter 1.20 mm.

tablet surface (c = 30.5 mm). This result demonstrates that under the prevailing hydrodynamic conditions the trough length behind the pores is quite small. In any case the troughs are not much longer than the visible length of about 2–3 mm. The turbulence generated by the presence of a pore is dampened quickly and the disturbed laminar flow is re-established within a short distance from the pore.

This finding was confirmed by the following experiment: parallel to the flow direction two rows of 8 pores each were drilled at equidistant intervals of 3 mm between the axis of succeeding pores (Fig. 6). The mean dissolution rate of that surface was 48.37 $\mu g \cdot s^{-1}$ (S.D. = 0.28 $\mu g \cdot s^{-1}$), which corresponds to an increase of the dissolution rate per pore, ΔR, of 0.14 ± 0.02 $\mu g \cdot s^{-1}$. The mean value of ΔR of the pores in Fig. 5 lying between 3 and 24 mm from the leading edge of the surface is 0.16 ± 0.04 $\mu g \cdot s^{-1}$. These ΔR values do not differ significantly ($P = 0.95$), so the pores lying downstream of other pores seem to act independently with respect to the increase of the dissolution rate. This is another indication that the turbulence provoked by a pore is dampened within about 2 mm under the prevailing hydrodynamic conditions in the parallel-plate dissolution cell.

Conclusions

The results obtained lead to the conclusion that the parallel-plate dissolution cell agrees with the theoretical predictions. In laminar flow the experimentally determined dissolution rate of a smooth surface agrees with theory in a wide range of hydrodynamic conditions. The measured critical pore diameter is in excellent accordance with the value predicted on basis of previous results obtained with the

rotating disk technique. Since a complete knowledge of the hydrodynamics in the parallel-plate cell is available, this apparatus provides a supplementary technique for studying the effects of pores on the dissolution rate next to the rotating disk method. It provides the opportunity of investigating pore effects at much lower Reynolds numbers without being subjected to natural convection.

References

Beek, W.J. and Muttzall, K.M.K., Transport Phenomena, John Wiley, New York, 1975, pp. 39–42.

Bird, R.B., Stewart, W.E. and Lightfoot, E.N., Transport Phenomena, John Wiley, New York, 1960, p. 47.

Brunt, K. and Bruins, C.H.P., Evaluation of the characteristics of the differential amperometric detector in combination with anion-exchange chromatography, using *l*-ascorbic acid as test compound, J. Chromatogr., 172 (1979) 37–47.

European Pharmacopoeia, 1st Edn., Maisonneuve, S.A., Sainte-Ruffine, France, 1975, Vol. III, pp. 133–134.

Grijseels, H. and de Blaey, C.J., Dissolution at porous interfaces. Int. J. Pharm., 9 (1981) 337–347.

Grijseels, H., Crommelin, D.J.A. and de Blaey, C.J., Hydrodynamic approach to dissolution rate. Pharm. Weekbl., Sci. Edn., 3 (1981) 129–144.

Grijseels, H., van Bloois, L., Crommelin, D.J.A. and de Blaey, C.J., Dissolution at porous interfaces II. A study of pore effects through rotating disk experiments. Int. J. Pharm., 14 (1983a) 299–311.

Grijseels, H., Crommelin, D.J.A. and de Blaey, C.J., Dissolution at porous interfaces III. Pore effects in relation to the hydrodynamics at a rotating disk surface. Int. J. Pharm., 14 (1983b) 313–323.

Grijseels, H., Harden, B.T.J.M. and de Blaey, C.J., Dissolution at porous interfaces IV. Pore effects in natural convection flow. Pharm. Weekbl., Sci. Edn., 5 (1983c) 88–94.

Ikenoya, S., Tsuda, T., Yamano, Y., Yamanishi, Y., Yamatsu, K., Ohmae, M., Kawabe, K., Nishino, H. and Kurahashi, T., Design and characterization of electrochemical detector for high-performance liquid chromatography and application to the determination of biogenic amines. Chem. Pharm. Bull., 26 (1978) 3530–3539.

Levich, V.G., Physicochemical Hydrodynamics, Prentice Hall, Englewood Cliffs, 1962, pp. 1–116.

Shah, A.C. and Nelson, K.G., Evaluation of a convective diffusion drug dissolution rate model. J. Pharm. Sci., 64 (1975) 1518–1520.

Swartzfager, D.G., Amperometric and differential pulse voltammetric detection in high performance liquid chromatography. Anal. Chem., 48 (1976) 2189–2192.

Wagenen, R.A., van, and Andrade, J.D., Flat plate streaming potential investigations: hydrodynamics and electrokinetic equivalency, J. Colloid Interface Sci., 76 (1980) 305–314.